Resonant light scattering induced by Coulomb interaction in semiconductor microstructures

1997 J. Phys.: Condens. Matter 9 4681

(http://iopscience.iop.org/0953-8984/9/22/020)

J. Phys.: Condens. Matter **9** (1997) 4681–4690. Printed in the UK PII: S0953-8984(97)79524-9

Resonant light scattering induced by Coulomb interaction in semiconductor microstructures

A O Govorov

Sektion Physik der Ludwig-Maximilians-Universität, Geschwister-Scholl-Platz 1, 80539 München, Germany, and Institute of Semiconductor Physics, Russian Academy of Sciences, Siberian Branch 630090, Novosibirsk-90, Russia

Received 13 November 1996, in final form 26 February 1997

Abstract. We consider inelastic light scattering by electron excitations in a two-dimensional electron system, which is induced by the Coulomb coupling between the Fermi sea and the interband excitons. The distinguishing feature of this mechanism of inelastic light scattering is a strong enhancement of the intensity in resonance with high two-dimensional subbands. Such resonant behaviour of the light scattering was observed in recent experiments for a two-dimensional electron plasma, quantum wires, and dots. In this paper we focus on the effect of the normal electric field on the intensity of the light scattering. We show that the interference between various virtual processes leads to the specific electric field dependence of the intensity. The intensity of the light scattering by charge-density excitations as a function of the normal electric field has a maximum at non-zero field. This maximum arises from the Coulomb direct interaction between the polarized exciton and the electron gas. Light scattering by spin-density excitations is assisted by the exchange interaction, and its intensity decreases with increasing electric field.

1. Introduction

Inelastic light scattering in semiconductor microstructures with relatively small numbers of electrons can be observed only under specific interband resonance conditions. In recent experiments on two-dimensional (2D) electron plasma [1–3], quantum wires, and dots [4, 5], light scattering by low-frequency intrasubband excitations was observed under conditions of resonance with *high 2D subbands*. In reference [6], the same resonant behaviour was found for light scattering by intersubband excitations. This type of resonant light scattering cannot be described by the use of the usual second-order perturbation theory, which predicts only resonance with the ground electron subband. To explain the resonant behaviour of the Raman intensity, the authors of reference [6] discussed third-order optical processes, which are assisted by the Coulomb interaction. Such processes are strongly enhanced under resonances with high 2D subbands. Before [6] appeared, third-order Raman processes in doped quantum wells were considered qualitatively in reference [7]. For bulk semiconductors, the third-order processes were widely discussed in connection with Raman scattering by optical phonons [8].

We note that in most cases Raman experiments are performed on GaAs–$Al_xGa_{1-x}As$ quantum wells with an internal normal electric field. In this paper, we suggest considering the effect of the normal electric field on the intensity. The electric field in a quantum well can arise from asymmetric doping, or can be induced by the voltage applied to a

0953-8984/97/224681+10$19.50

metallic gate on the top of a sample. In addition, built-in electric fields can arise in strained semiconductor layers due to the piezoelectric effect.

In the present paper, we propose a quantitative description for the third-order Raman processes in a quasi-2D electron plasma of a quantum well in the regime of resonance of the conduction and valence bands. We focus only on light scattering by low-frequency intrasubband excitations, and on interband resonances between 2D subbands with equal numbers. Using model calculations, we show that the electric field dependence of the intensity reflects the interference between various virtual processes. In a square quantum well, the main resonant contribution to the intensity can be connected with the Coulomb exchange interaction. In the presence of an electric field, the exciton forms a dipole, which strongly interacts with an electron gas, and can create charge-density excitations. Such Coulomb direct interaction results in a maximum in the electric field dependence of the intensity of the light scattering by charge-density excitations.

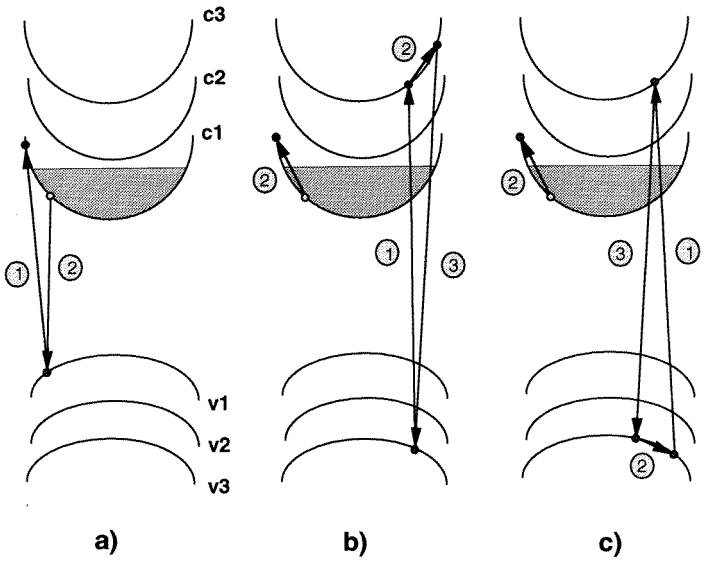

Figure 1. (a) The second-order scattering process involving two interband optical transitions; this process is enhanced by resonance with the ground exciton. (b), (c) Third-order scattering processes, which involve either a photo-excited electron (b) or a hole (c); the interband processes are optical, while the intraband transitions are induced by the Coulomb interaction. The processes (b) and (c) are strongly enhanced by resonance with high subbands.

2. Third-order light scattering processes

In this section we intend to consider the processes of light scattering by low-frequency intrasubband excitations of a quasi-2D electron system under interband resonance conditions. The second-order optical process corresponds to the diagram shown in figure 1(a), where the interband transitions between the conduction and valence bands are assisted by incident and scattered photons, $\omega_{1\,(2)}$. The cross section in this case has the resonant factor $1/(\omega_1 - E_g)^2$ [9], where E_g is the energy of interband resonance involving the ground 2D subbands in the conduction and valence bands. To include resonances with high 2D subbands, we suggest considering the diagrams shown in figures 1(b), 1(c). In these diagrams, interband transitions

are assisted by incident and scattered photons, while intrasubband transitions are induced by the Coulomb coupling between a photo-excited electron–hole pair (or an exciton) and the plasma. The first and third virtual processes are optical, while the intermediate virtual process is assisted by the Coulomb coupling. The two processes shown in figure 1(b), 1(c) involve either a photo-excited electron or a hole. These diagrams give the main contributions to the cross section if the photon energy is close to resonance. Also, we assume that the characteristic energy of the intrasubband excitations ω is much less than the intersubband spacing Ω. In this case we have the situation in which both incident and scattered photons are in resonance with high subbands of a quantum-well system. Usually, the intrasubband energies ω are of order 2–3 meV, while the intersubband spacing $\Omega \simeq$ 10–20 meV. If $\omega \ll \Omega$, we can consider isolated interband resonance with certain high subbands in the conduction and valence bands.

To calculate the interband optical matrix elements for a GaAs quantum well, we will use the Bloch functions of the Kane model. Also, we will consider a simple parabolic model of the valence band, and resonance with a heavy-hole subband. The envelope wave functions of the conduction band can be written as $\Psi_n^c(\boldsymbol{R}) = \mathrm{e}^{\mathrm{i}\boldsymbol{p}\cdot\boldsymbol{r}}\chi_n^c(z)$, where $\boldsymbol{R} = (\boldsymbol{r}, z)$ is the 3D coordinate, and $\boldsymbol{r}$ and z are the in-plane and normal coordinates, respectively; $\chi_n^c(z)$ is the size-quantization wave function, and n is the number of the 2D subband. The single-electron wave function, written taking into account the Bloch part, is $\Psi_n^c(\boldsymbol{R})u_\sigma^c(\boldsymbol{R})$. Here the Bloch part $u_\sigma^c(\boldsymbol{R}) = |S\rangle|\sigma\rangle$, where $|S\rangle$ is the spatially periodic function and $|\sigma\rangle$ is the spin function with $\sigma = \pm 1/2$. The ground subband in the conduction band has the index $n = 0$. The envelope wave functions of the heavy-hole subbands can be written in a similar form: $\Psi_m^v(\boldsymbol{R}) = \mathrm{e}^{\mathrm{i}\boldsymbol{p}\cdot\boldsymbol{r}}\chi_m^v(z)$, where $\chi_m^v(z)$ is the size-quantization wave function for a 2D subband numbered m. The total wave function of a heavy hole is $\Psi_m^v(\boldsymbol{R})u_{J_z}^v(\boldsymbol{R})$, where $u_{J_z}^v(\boldsymbol{R})$ are the Bloch functions with the angular momenta $J_z = \pm 3/2$. The Bloch functions of heavy holes in the Kane model are $u_{+3/2}^v(\boldsymbol{R}) = |X + \mathrm{i}Y\rangle|\uparrow\rangle/\sqrt{2}$ and $u_{-3/2}^v(\boldsymbol{R}) = |X - \mathrm{i}Y\rangle|\downarrow\rangle/\sqrt{2}$.

The cross section of the inelastic light scattering is given by (see [9])

$$\frac{\mathrm{d}^2\sigma}{\mathrm{d}\Omega\ \mathrm{d}\omega} = \frac{\omega_2}{\omega_1}\frac{e^4}{c^4 m_0^4}S(\omega) \qquad S(\omega) = \sum_F |\langle F|\hat{V}_{eff}|I\rangle|^2\delta(E_F - E_I - \omega) \tag{1}$$

where $S(\omega)$ is the structure factor, and $\omega_{1\,(2)}$ and $\boldsymbol{k}_{1\,(2)}$ are the energies and the wave vectors of incident (scattered) photons, respectively; $\omega = \omega_1 - \omega_2$ is the energy transfer; $\hat{V}_{eff}$ is the effective operator of the light scattering, which describes the transition between the many-electron initial state $|I\rangle$ of the energy E_I and the final state $|F\rangle$ of the energy E_F. The temperature is assumed to be zero.

In a many-particle system, the matrix elements for the light scattering can be written as

$$\hat{V}_{eff} = \sum_{p,\sigma_f,\sigma_i} M(\boldsymbol{p}, \sigma_f, \sigma_i)\hat{c}^+_{p+k_{||},\sigma_f}\hat{c}_{p,\sigma_i} \tag{2}$$

where $\hat{c}^+_{p,\sigma}$ and $\hat{c}_{p,\sigma}$ are the creation and annihilation operators for the lowest electron subband; $\boldsymbol{p}$ and σ are the 2D electron momentum and the spin, respectively. The matrix element $M(\boldsymbol{p}, \sigma_f, \sigma_i)$ describes a single-particle intrasubband transition $|\boldsymbol{p}, \sigma_i\rangle \rightarrow |\boldsymbol{p} + \boldsymbol{k}_{||}, \sigma_f\rangle$ in a plasma, where $\boldsymbol{k}_{||} = \boldsymbol{k}_{1||} - \boldsymbol{k}_{2||}$ is the light momentum transfer parallel to the layer. To write out the operator (2), we have taken into account the conservation of the in-plane momentum in a 2D system. In addition, we assume that electrons in the initial state occupy only the ground subband in the conduction band.

The resonant structure of the cross section depends on the character of the intermediate states. The intermediate states for the light scattering process can be taken in the form of

an electron–hole pair, or in the form of an exciton. In the following we will discuss both cases.

The optical processes shown in figures 1(b), 1(c) are described by a third-order perturbation theory. As was mentioned above, the equilibrium electron gas occupies the ground 2D subband, while the photo-excited electron–hole (or the exciton) relates to high 2D subbands. In our approach, the Coulomb interaction between the photo-excited electron–hole pair (or the exciton) and the electron gas of the ground subband in the conduction band will be considered in the framework of a perturbation theory. On the other hand, in the case of the excitonic intermediate states, the Coulomb coupling between an electron and a hole in the photo-generated exciton will not be treated as a perturbation.

We will calculate the cross section of the light scattering in two steps. In the first step of our calculations, we will find the matrix elements $M(\boldsymbol{p}, \sigma_f, \sigma_i)$ for a non-interacting electron gas of the ground subband. In the second step, using the matrix elements $M(\boldsymbol{p}, \sigma_f, \sigma_i)$, we will express the cross section (1) in terms of the correlation functions of an interacting electron gas. A similar procedure was used before in [9, 10], to describe the second-order Raman processes in doped semiconductors. This method is based on the assumption that the Coulomb coupling in the electron gas can be considered as a perturbation.

2.1. Processes involving electron–hole pairs

The matrix elements for the processes shown in figures 1(b), 1(c) can be written as

$$M(\boldsymbol{p}, \sigma_f, \sigma_i) = \sum_{\nu',\nu} \frac{\langle f|\boldsymbol{A}_2 \cdot \hat{\boldsymbol{p}}|\nu'\rangle\langle\nu'|\hat{U}|\nu\rangle\langle\nu|\boldsymbol{A}_1 \cdot \hat{\boldsymbol{p}}|i\rangle}{(E_f - E_{\nu'} + \omega_2)(E_i - E_\nu + \omega_1)} \tag{3}$$

where $|i\rangle$ and $|f\rangle$ are the initial and final states, respectively; $|\nu\rangle$ and $|\nu'\rangle$ are intermediate states, $E_{i,\nu,\nu',f}$ are the energies of the corresponding states, and $\hat{U}$ is the Coulomb interaction potential; $\boldsymbol{A}_{1\,(2)}$ are the vector potentials of incident (scattered) photons, and $\hat{\boldsymbol{p}}$ is the momentum.

It is convenient to calculate the matrix elements (3) by use of the second-quantization formalism. As was mentioned above, the matrix element $M(\boldsymbol{p}, \sigma_f, \sigma_i)$ describes a single-electron transition in a non-interacting gas. The initial state $|i\rangle$ in equation (3) relates to the equilibrium non-interacting Fermi gas on the ground subband. The final state in equation (3) should include a single-electron excitation in a plasma and, thus, can be written as $|f\rangle = \hat{c}^+_{p+k_{||},\sigma_f}\hat{c}_{p,\sigma_i}|i\rangle$. The interband optical matrix elements in equation (3) involve the Bloch functions and can be written as

$$\boldsymbol{A}_1 \cdot \hat{\boldsymbol{p}} = \frac{P_{cv}}{\sqrt{2}}\langle\chi^c_n|\mathrm{e}^{\mathrm{i}k_{1z}z}|\chi^v_m\rangle \sum_q \hat{a}^+_{q+k_{1||},n,+1/2}\hat{b}_{q,m,+3/2}(e_{1x} + \mathrm{i}e_{1y}) + \hat{a}^+_{q+k_{1||},n,-1/2}\hat{b}_{q,m,-3/2}(e_{1x} - \mathrm{i}e_{1y}) \tag{4a}$$

$$\boldsymbol{A}_2 \cdot \hat{\boldsymbol{p}} = \frac{P^*_{cv}}{\sqrt{2}}\langle\chi^v_m|\mathrm{e}^{-\mathrm{i}k_{2z}z}|\chi^c_n\rangle \sum_q \hat{b}^+_{q-k_{2||},m,+3/2}\hat{a}_{q,n,+1/2}(e_{2x} - \mathrm{i}e_{2y}) + \hat{b}^+_{q-k_{2||},m,-3/2}\hat{a}_{q,n,-1/2}(e_{2x} + \mathrm{i}e_{2y}) \tag{4b}$$

where $\hat{a}^+_{q,n,\pm1/2}$ and $\hat{b}^+_{q,m,\pm3/2}$ are the creation operators for electrons of the high subbands numbered n and m in the conduction and valence bands, respectively; P_{cv} is the interband matrix element in the Kane model, and $\boldsymbol{e}_1$ and $\boldsymbol{e}_2$ are the polarizations of the incident and scattered photons, respectively. The matrix elements (4) are spin dependent, and describe the allowed interband transitions: $u^v_{+3/2} \to u^c_{+1/2}$ and $u^v_{-3/2} \to u^c_{-1/2}$. The intermediate states

$|\nu\rangle$ and $|\nu'\rangle$ include a photo-excited electron–hole pair related to the high 2D subbands numbered n and m. For example, the intermediate state $|\nu\rangle$ can be written in the form $|\nu\rangle = \hat{a}^{+}_{q+k_{1||},n,\pm 1/2}\hat{b}_{q,m,\pm 3/2}|i\rangle$. The virtual transition between the intermediate states $|\nu\rangle$ and $|\nu'\rangle$ is induced by the Coulomb coupling. In our calculations we take into account the Coulomb direct and exchange interactions between the photo-excited electron and the Fermi gas. At the same time, we assume that the photo-excited valence hole is coupled with the Fermi gas only by Coulomb direct interaction. The exchange interaction between a valence-band hole and electrons of the conduction band is neglected because such an interaction involves mixing between the orthogonal short-period Bloch wave functions by the long-range Coulomb coupling. Thus, we believe that the amplitudes of the interband exchange interaction include a small parameter proportional to the lattice constant.

To demonstrate the distinctive features of third-order Raman scattering, we now focus on the case of interband resonances between 2D subbands with the same indices. Such resonant conditions were used in the experimental work described in [3]. In order to calculate the third-order matrix element (3), we have to take into account the following facts: (i) all of the matrix elements in equation (3) conserve the total momentum of the system; and (ii) the intermediate states in equation (3) can be electron–hole pairs with two possible spin combinations: ($\sigma = +1/2, J = +3/2$) and ($\sigma = -1/2, J = -3/2$) (see equation (4)). Thus, by using equations (3), (4), we find the third-order matrix elements for resonances with $n = m$:

$$M(\boldsymbol{p}, \sigma_f, \sigma_i) = \frac{P_{cv}^2 B_{nn}}{2} \sum_{\tilde{p}} \left(\frac{(\boldsymbol{e}_{1||} \cdot \boldsymbol{e}_{2||})[2U_{cc}(k_{||}) - 2U_{cv}(k_{||}) - U_{cc}^{exc}(\tilde{\boldsymbol{p}} - \boldsymbol{p})]}{(E_{nn} + \tilde{p}^2/2\mu - \omega_1)^2} + \frac{\mathrm{i}\, 2\sigma_i [\boldsymbol{e}_1 \times \boldsymbol{e}_2]_z U_{cc}^{exc}(\tilde{\boldsymbol{p}} - \boldsymbol{p})}{(E_{nn} + \tilde{p}^2/2\mu - \omega_1)^2} \right) \delta_{\sigma_i, \sigma_f} \tag{5}$$

where $\sigma_i = \sigma_f = \pm 1/2$, $1/\mu = 1/m_c + 1/m_v$, $m_{c\,(v)}$ are the effective masses of electrons (holes) and E_{nn} is the interband resonance energy; $(\boldsymbol{e}_{1||} \cdot \boldsymbol{e}_{2||})$ and $[\boldsymbol{e}_1 \times \boldsymbol{e}_2]$ are scalar and vector products, respectively; the factor

$$B_{nn} = \langle \chi_n^v | \mathrm{e}^{-\mathrm{i}k_{2z}z} | \chi_n^c \rangle \langle \chi_n^c | \mathrm{e}^{\mathrm{i}k_{1z}z} | \chi_n^v \rangle \tag{6}$$

describes the overlap between the electron and hole wave functions. The matrix elements (5) are spin dependent because of the spin–orbit structure of the valence band. In addition, one can see from equation (5) that the processes involving the heavy-hole band conserve the spin. The matrix elements of the Coulomb interaction in equation (5) are given by

$$\begin{aligned} U_{cc}(k) &= \iint \Psi_0^c(z)\Psi_0^c(z) U_k(z - z') \Psi_n^c(z')\Psi_n^c(z')\, \mathrm{d}z\, \mathrm{d}z' \\ U_{cv}(k) &= \iint \Psi_0^c(z)\Psi_0^c(z) U_k(z - z') \Psi_n^v(z')\Psi_n^v(z')\, \mathrm{d}z\, \mathrm{d}z' \\ U_{cc}^{exc}(\tilde{\boldsymbol{p}} - \boldsymbol{p}) &= \iint \Psi_0^c(z)\Psi_n^c(z) U_{\tilde{p}-p}(z - z') \Psi_0^c(z')\Psi_n^c(z')\, \mathrm{d}z\, \mathrm{d}z' \end{aligned} \tag{7}$$

where $U_k(z - z') = [(2\pi e^2)/(\epsilon k)]\mathrm{e}^{-k|z-z'|}$ is the 2D Fourier transform of the Coulomb potential. The equations (5) and (7) were written assuming $k_{||} \ll p$, where $p \sim p_f$ and p_f is the Fermi wave vector. The matrix elements $U_{cc\,(cv)}$ relate to the Coulomb direct interaction between the photo-excited electron (hole) and the Fermi sea, while U_{cc}^{exc} is connected with the exchange interaction in the conduction band. The contributions of the direct Coulomb interaction $U_{cc\,(cv)}$ in equation (5) have opposite signs because an electron–hole pair is neutral. We note also that the combination $U_{cc}(k_{||}) - U_{cv}(k_{||})$ remains finite in the limit $k_{||} \to 0$. The spin-dependent and spin-independent terms in equation (5) lead

to spin- and charge-density excitation spectra, respectively. The spin-dependent term in equation (5) is induced only by the exchange interaction [6], because the Coulomb direct interaction does not involve spins. The amplitude of the spin-independent processes (the first term in equation (5)) includes the combination $2(U_{cc} - U_{cv}) - U_{cc}^{exc}$, and arises from both types of the Coulomb interaction. The resonant behaviour of the amplitude can be seen after taking the integral over $\tilde{p}$ in equation (5), and it is mostly determined by the function $1/(E_{nn} - \omega_1)$. We note that all of the qualitative results obtained here are also valid for resonances with the light-hole and split-off valence bands.

To analyse quantitatively the electric field dependence of the cross section, we consider the case of the exciton intermediate states.

2.2. Processes involving excitons

It was found experimentally [3, 6] that there are very narrow peaks in the resonant structure of the cross section. These peaks correspond to the high subband excitons. In order to model light scattering induced by the Coulomb coupling with excitons, we have to find the matrix elements (3), taking into account the excitonic character of intermediate states. The envelope wave function of an exciton can be written in the simplified form $\Psi_{nn}^{exc}(R_e, R_h) = \mathrm{e}^{\mathrm{i}\boldsymbol{P}_{exc}\boldsymbol{R}_{exc}}\Psi_n^c(z_e)\Psi_n^v(z_h)\phi(\boldsymbol{r}_e - \boldsymbol{r}_h)$ [11], where $(\boldsymbol{r}_e, z_e)$ and $(\boldsymbol{r}_h, z_h)$ are the coordinates of an electron and a hole, respectively; $\boldsymbol{R}_{exc} = (m_c\boldsymbol{r}_e + m_v\boldsymbol{r}_h)/M$ is the centre-of-mass coordinate of an exciton, $M = m_c + m_v$, P_{exc} in the exciton momentum, and the indices nn show the subband numbers. The intermediate state $|\nu\rangle$ in equation (3) is described now by the following wave function [11]:

$$|\nu\rangle = \sum_q \phi(q)\hat{a}^+_{\boldsymbol{q}+(m_c/M)\boldsymbol{k}_{1||},n,\pm 1/2}\hat{b}_{\boldsymbol{q}-(m_v/M)\boldsymbol{k}_{1||},n,\pm 3/2}|i\rangle$$

where $\phi(q)$ is the Fourier transform of the function $\phi(r)$. For the case of excitons, the interband optical matrix elements are given by equation (4) with an additional factor which, in the limit $k_{1\,(2)||}a \ll 1$, is equal to $\phi(0)$ [11], where a is the Bohr radius. The matrix element of the Coulomb interaction in equation (3) describes a virtual-exciton transition $\boldsymbol{P}_{exc} \to \boldsymbol{P}_{exc} - \boldsymbol{k}_{||}$ with the creation of a single-particle excitation $\boldsymbol{p} \to \boldsymbol{p} + \boldsymbol{k}_{||}$ in the electron plasma. Thus, after calculations we have

$$M(\boldsymbol{p}, \sigma_f, \sigma_i) = \frac{P_{cv}^2 B_{nn}}{2}\frac{\phi^2(0)}{(E_{nn} - \omega_1)^2}\{(\boldsymbol{e}_{1||}\cdot\boldsymbol{e}_{2||})[2U_{cc}(k_{||}) - 2U_{cv}(k_{||}) - V_{cc}^{exc}(p)] + \mathrm{i}\,2\sigma_i[\boldsymbol{e}_1\times\boldsymbol{e}_2]_z V_{cc}^{exc}(p)\}\delta_{\sigma_i,\sigma_f}. \tag{8}$$

Here $\sigma_i = \sigma_f = \pm 1/2$ and E_{nn} is the exciton energy. Equation (8) is written for $k_{1\,(2)||}a \ll 1$. The matrix element of the exchange interaction between an exciton and a free electron is

$$V_{cc}^{exc}(p) = \sum_q \phi^2(q)U_{cc}^{exc}(\boldsymbol{q} - \boldsymbol{p}). \tag{9}$$

One can see that the resonant enhancement for an excitonic intermediate state is stronger than that for an electron–hole pair because of the discrete character of the exciton spectrum. Also, the excitonic character of wave functions results in the additional factor $\phi^2(0)$ in the amplitude, and changes the matrix element of the exchange interaction.

3. Discussion

One can see from the expressions for $M(\boldsymbol{p}, \sigma_f, \sigma_i)$ (equations (5), (8)) that the electric field dependence of the amplitude can reflect the interference between virtual channels of

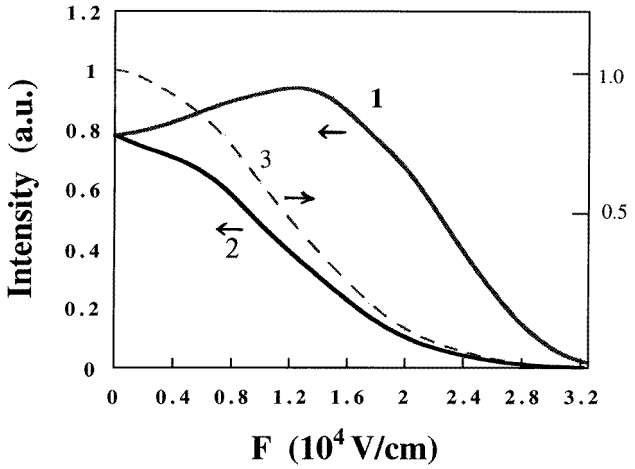

Figure 2. The electric field dependences of the cross section in a 200 Å quantum well, based on GaAs, for the interband excitonic resonance with $n = m = 3$; the in-plane momentum is $k_{||} = 5 \times 10^4$ cm^{-1}, the 2D electron density is 5×10^{11} cm^{-2}, and the photon energy is about 1.6 eV. Curves 1 and 2 show the functions $A_e(F)$ and $A_s(F)$, respectively. Curve 3 shows the overlap factor $|B_{33}(F)|^2$.

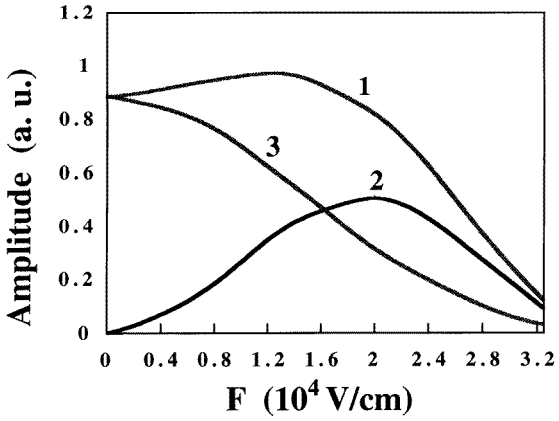

Figure 3. The amplitude of the light scattering by charge-density excitations, and its components as functions of the normal electric field: curve 1 shows the total amplitude $2(U_{cc} - U_{cv}) - U_{cc}^{exc}$; curves 2 and 3 represent the functions $2(U_{cc} - U_{cv})$ and $-U_{cc}^{exc}$, respectively. The parameters are similar to those for figure 2.

scattering. In a square quantum well with infinitely high walls, the wave functions $\Psi_n^{c\,(v)}$ do not depend on the effective masses and, consequently, $\Psi_n^c = \Psi_n^v$. In this case, for interband resonances with $n = m$, the value $U_{cc} - U_{cv} = 0$, and hence the light scattering arises only from the exchange interaction. Thus, in a square well, the direct-interaction contribution is absent, and the amplitude is induced by the exchange interaction. The situation is changed in a normal electric field, when the exciton has a non-zero dipole moment and can induce charge-density excitations in a Fermi sea due to the direct interaction. Thus, we can expect that the direct Coulomb interaction contribution $(U_{cc} - U_{cv})$ can be crucial if the quantum

well is tilted. These qualitative conclusions are supported by the numerical results shown in figures 2 and 3. The cross section was calculated for the excitonic resonance with $n = m = 3$ in a 200 Å quantum well. This resonance was observed in reference [3] in the resonant structure of Raman scattering by 2D plasmons. The exciton wave function $\phi(r)$ is taken in the simplest 2D form [11]: $\phi(r) = a^{-1}(8/\pi)^{1/2}\exp(-2r/a)$, where a is the Bohr radius of GaAs. The exchange-interaction matrix elements are relatively insensitive to the value of a, which was chosen to be 140 Å. The wave functions $\Psi_n^{c\,(v)}$ were calculated for a quantum well with the uniform normal electric field $\boldsymbol{F}||\boldsymbol{z}$ and infinitely high walls (no penetration into the barriers). In this simplest model of a quantum well, the $\Psi_n^{c\,(v)}$ are expressed in terms of the Airy functions.

Now we focus on the electric field dependence of the light scattering intensity, which is determined by the F-dependent coefficients in equation (8). The cross section of the light scattering includes the second power of these coefficients, and will be written down later. One can see from equation (8) that the intensity of the light scattering by charge-density excitations (a spin-independent process) is proportional to the factor

$$A_e(F) = |B_{nn}|^2[2(U_{cc} - U_{cv}) - V_{cc}^{exc}(p)]^2. \tag{10}$$

The cross section of the spin-dependent light scattering is connected only with the exchange interaction, and includes the factor

$$A_s(F) = |B_{nn}|^2[V_{cc}^{exc}(p)]^2. \tag{11}$$

In these factors we can choose $p = p_f$. For typical conditions in experiments, the factors A_e and A_s as a function of F are shown in figure 2. Here we choose back-scattering geometry with $k_{||} = 5 \times 10^4$ cm^{-1}. The change of the wave vector $k_{||}$ does not lead to a major effect on the intensity. Figure 2 shows that the intensity of the light scattering by charge-density excitations (the function A_e) is maximal for non-zero electric field, where the Coulomb direct interaction becomes important. The intensity of the light scattering by spin-density excitations (the function A_s) is a decreasing function of the electric field. The decrease of all of the intensities at high electric fields is connected with the overlap factor $|B_{nn}|^2$, which rapidly drops with increasing electric field. Figure 3 shows how the direct and exchange interactions contribute to the amplitude A_e at various electric fields. One can see that in low electric fields the exchange-interaction contribution dominates, while for $F > 1.6 \times 10^4$ V cm^{-1} the direct interaction plays the main role. In addition, we have calculated the factors A_e and A_s for the case of $n = m = 2$ interband resonance. We have found that these factors for the case where $n = m = 2$ are bigger than those for $n = m = 3$ by a few times, but the F-dependence remains qualitatively similar.

We now turn to the cross section of the light scattering (see equation (1)). Using the matrix elements (8), we can write the effective operator of the light scattering (2) as a linear combination of the operators of charge and spin densities, $\hat{\rho}_e(\boldsymbol{k}_{||}) = \sum_{p,\sigma}\hat{c}^+_{p+k_{||},\sigma}\hat{c}_{p,\sigma}$ and $\hat{\rho}_s(\boldsymbol{k}_{||}) = \sum_{p,\sigma}\sigma\hat{c}^+_{p+k_{||},\sigma}\hat{c}_{p,\sigma}$. In the next step, we can express the cross section in terms of the charge- and spin-density correlation functions, which describe the charge- and spin-density excitation spectra of the light scattering [9]. Thus, using equations (1), (2), (8), we obtain

$$S(\omega) = \frac{P_{cv}^4\phi^4(0)}{4(E_{nn} - \omega_1)^4}[(\boldsymbol{e}_{1||}\cdot\boldsymbol{e}_{2||})^2 A_e F_e(\omega, k_{||}) + [\boldsymbol{e}_1 \times \boldsymbol{e}_2]_z^2 A_s F_s(\omega, k_{||})] \tag{12}$$

where $F_e(\omega, k_{||})$ and $F_s(\omega, k_{||})$ are the charge- and spin-density correlation functions, respectively. Analytic expressions for the correlation functions of a 2D system can be

found in references [12, 13]:

$$F_e = \frac{k\omega_p(k_{||})}{4}\delta(\omega - \omega_p) \qquad F_s = \frac{m_c}{\pi^2}\frac{\omega}{\sqrt{(k_{||}v_f)^2 - \omega^2}} \qquad \omega < k_{||}v_f \tag{13}$$

where $\omega_p(k_{||}) \propto \sqrt{k_{||}}$ is the 2D plasmon frequency, and v_f is the Fermi velocity.

The intensities related to charge- and spin-density excitations are proportional to the factors $(\boldsymbol{e}_{1||} \cdot \boldsymbol{e}_{2||})^2$ and $[\boldsymbol{e}_1 \times \boldsymbol{e}_2]_z^2$, respectively. These combinations of the polarization vectors determine the selection rules of the light scattering [9]. In conventional back-scattering geometry, the charge- and spin-density excitation spectra can be easily separated by the use of appropriate combinations of the polarizations of incident and scattered photons [1, 6].

Usually, the in-plane wave vector $k_{||}$ is much less than $1/L$, where L is the quantum-well width. Thus, the factors $A_{e\,(s)}$ can be taken for zero light momentum, and the $k_{||}$-dependence of the intensity arises mostly from the correlation functions $F_{e\,(s)}$. In the case of light scattering by plasmons, the intensity becomes proportional to $k_{||}^{3/2}$. A strong $k_{||}$-dependence of the cross section related to 2D plasmons was noted in the experimental work described in references [1, 3]. Another distinctive feature of this scattering mechanism is the magnetic field dependence of the intensity. The perpendicular magnetic field can suppress light scattering, as was observed in the experiment described in [14]. In a high magnetic field, the matrix element of the operator $\hat{\rho}_e(\boldsymbol{k}_{||})$ for the inter-Landau-level electron transition $\Delta l = 1$ is proportional to $k_{||}l_c$, where l is the Landau-level number, l_c is the magnetic length, and $k_{||}l_c \ll 1$. Thus, the cross section is proportional to $(k_{||}l_c)^2 \propto 1/B$ [15], and decreases with increasing magnetic field.

One of the first experimental observations of Raman scattering by in-plane electron excitations [17] relates to GaAs–AlAs heterostructures, in which the spectrum of the valence band is continuous. The resonant Raman measurements in reference [17] were performed slightly above the fundamental gap. This resonant behaviour shows that the light scattering observed in the work described in [17] could be connected with the third-order optical processes.

The third-order Coulomb-interaction-induced mechanism can also play a role in Raman studies of electronic quantum dots and wires [4, 5]. This mechanism allows the observation of resonant Raman scattering in the regime of the laser energies above the fundamental gap. In this regime, Raman spectra are located far away from intensive photoluminescence lines. In many particular cases, the lateral size of a microstructure is much greater than the quantum-well width, and so the lateral confinement essentially does not change the structure of the interband resonances in the system. In this case we can use the results of the present paper, which were obtained for a 2D system. For example, we can apply our results to the case of relatively wide electron wires, where the single-electron spectrum and interband resonances are mostly similar to those in a quantum well. At the same time, the plasmon spectrum in such wires can be strongly modified, and can consist of confined modes [16]. To describe the light scattering in this case, we can use equation (12) with a modified correlation function, which includes a set of δ-functions due to the confined-mode structure of the plasmon spectrum.

In conclusion, we have discussed the k-dependent mechanism of light scattering, which can be responsible for the resonant structure of light scattering observed in recent experiments. The mechanism is assisted by Coulomb interaction in intermediate states, and is enhanced by resonances with high 2D subbands. The intensity of the light scattering depends in a specific way on the internal electric field in a quantum well, because of the interference between virtual processes. In the case of light scattering by charge-density

excitations, the intensity is maximal in the non-zero electric field when the Raman process is induced by the interaction between the dipole moment of an exciton and the electron gas. The amplitude of light scattering by spin-density excitations is proportional to the matrix element of the Coulomb exchange interaction, and is maximal at zero electric field.

Acknowledgments

The author would like to thank B Jusserand, A Pinczuk, A Schmeller, W Hansen, and A Förster for helpful discussions. This work was supported by INTAS and the A von Humboldt Stiftung.

References

[1] Jusserand B, Richards D, Fasol G, Weimann G and Schlapp W 1990 *Surf. Sci.* **229** 394
[2] Jusserand B, Richards D, Allan G, Priester C and Etienne B 1995 *Phys. Rev.* B **51** 4707
[3] Förster A, Schmeller A, Hansen W, Kotthaus J P, Klein W, Böhm G, Tränkle G and Weimann G 1995 *Proc. Workshop on Highlights of Light Spectroscopy on Semiconductors (Rome, 1995)* ed A D'Andrea and L G Quagliano (Singapore: World Scientific) p 183
Förster A 1995 *Diploma Thesis* LMU München
[4] Schmeller A, Goñi A R, Pinczuk A, Weiner J S, Calleja J M, Dennis B S, Pfeiffer L N and West K W 1994 *Solid-State Electron.* **37** 1281
[5] Lockwood D J, Hawrylak P, Wang P D, Song Y P, Sotomayor Torres C M, Holland M C, Pinczuk A and Dennis B S 1996 *Solid-State Electron.* **40** 339
[6] Danan G, Pinczuk A, Valladares J P, Pfeiffer L N, West K W and Tu C W 1989 *Phys. Rev.* B **39** 5512
[7] Burstein E, Pinczuk A and Mills D I 1980 *Surf. Sci.* **98** 451
[8] Pinczuk A and Burstein E 1975 *Light Scattering in Solids* ed M Cardona (Berlin: Springer) pp 23–75
[9] Hamilton D C and McWhorter A L 1969 *Light Scattering Spectra of Solids* ed G B Wright (New York: Springer) p 309
[10] Blum F A 1970 *Phys. Rev.* B **1** 1125
[11] Haug H and Koch S W 1990 *Quantum Theory of the Optical and Electronic Properties of Semiconductors* (Singapore: World Scientific) pp 148–76
[12] Stern F 1967 *Phys. Rev. Lett.* **18** 546
[13] Govorov A and Chaplik A V 1989 *Sov. Phys.–JETP* **67** 2532
Chaplik A V and Govorov A O 1990 *Superlatt. Microstruct.* **7** 161
[14] Worlock J M, Pinczuk A, Tien Z J, Perry C H, Störmer H, Dingle R, Gossard A C, Wiegmann W and Aggarwal R L 1981 *Solid State Commun.* **40** 867
[15] Govorov A O and Chaplik A V 1993 *Solid State Commun.* **85** 827
[16] Strenz R, Rosskopf V, Hirler F, Abstreiter G, Böhm G, Tränkle G and Weimann G 1994 *Semicond. Sci. Technol.* **9** 399
[17] Fasol G, Mestres N, Hughes H P, Fischer A and Ploog K 1986 *Phys. Rev. Lett.* **56** 2517